Surface Science, 600 (2006), 983-994

In-situ XPS study of Pd(111) oxidation, *Part 1: 2D oxide formation in 10^{-3} mbar O_2*

D. Zemlyanov[a*], B. Aszalos-Kiss[a], E. Kleimenov[b], D. Teschner[b], S. Zafeiratos[b], M. Hävecker[b], A. Knop-Gericke[b], R. Schlögl[b], H. Gabasch[c], W. Unterberger[c], K. Hayek[c], B. Klötzer[c]

[a]Materials and Surface Science Institute and Physics Department, University of Limerick, Limerick, Ireland
[b]Abteilung Anorganische Chemie, Fritz-Haber-Institut der Max-Planck-Gesellschaft, Faradayweg 4-6, D-14195 Berlin, Germany
[c]Institut für Physikalische Chemie, Universität Innsbruck, A-6020, Innsbruck, Austria

[*] Corresponding author: e-mail dimazemlyanov@purdue.edu, Purdue University Birck Nanotechnology Center (BRCK), 1205 West State Street West Lafayette, IN 47907-2057, USA

Received: 3 october 2005, accepted for publication 12 december 2005, available online 13 january 2006

Abstract

The oxidation of the Pd(111) surface was studied by *in situ* XPS during heating and cooling in 3×10^{-3} mbar O_2. A number of adsorbed/dissolved oxygen species were identified by *in situ* XPS, such as the 2 dimensional surface oxide (Pd_5O_4), the supersaturated O_{ads} layer, dissolved oxygen and the $(\sqrt{67}\times\sqrt{67})$R12.2° surface structure.

Exposure of the Pd(111) single crystal to 3×10^{-3} mbar O_2 at 425 K led to formation of the 2D oxide phase, which was in equilibrium with a super-saturated O_{ads} layer. The supersaturated O_{ads} layer was characterized by the O 1s core level peak at 530.37 eV. The 2D oxide, Pd_5O_4, was characterized by two O 1s components at 528.92 eV and 529.52 eV and by two oxygen-induced Pd $3d_{5/2}$ components at 335.5 eV and 336.24 eV. During heating in 3×10^{-3} mbar O_2 the supersaturated O_{ads} layer disappeared whereas the fraction of the surface covered with the 2D oxide grew. The surface was completely covered with the 2D oxide between 600 K and 655 K. Depth profiling by photon energy variation confirmed the surface nature of the 2D oxide. The 2D oxide decomposed completely above 717 K. Diffusion of oxygen in the palladium bulk occurred at these temperatures. A substantial oxygen signal assigned to the dissolved species was detected even at 923 K. The dissolved oxygen was characterised by the O 1s core level peak at 528.98 eV. The "bulk" nature of the dissolved oxygen species was verified by depth profiling.

During cooling in 3×10^{-3} mbar O_2, the oxidised Pd^{2+} species appeared at 788 K whereas the 2D oxide decomposed at 717 K during heating. The surface oxidised states exhibited an inverse hysteresis. The oxidised palladium state observed during cooling was assigned to a new oxide phase, probably the $(\sqrt{67}\times\sqrt{67})$R12.2° structure.

1. Introduction

Palladium is widely used as a catalyst in a number of oxidation reactions such as complete oxidation of hydrocarbons in automotive exhausts and total methane combustion for gas-powered turbines. In comparison to other metals, palladium shows the highest rate per unit metal surface for methane oxidation [1]. Catalytic combustion is carried out under conditions varying from low temperatures, where PdO is the thermodynamically stable phase, to high temperatures, where Pd metal is stable. PdO is believed to be the more active phase in methane combustion than metallic Pd [2-4].

A number of research groups [5-10] observed that the combustion rates are different when the catalyst is either cooled or heated in the reaction mixture. This unusual kinetic behaviour, referred to as an activity hysteresis, was assigned to the decomposition of PdO to Pd and its re-formation [5, 9]. It was suggested that strongly bound chemisorbed oxygen forms on the palladium surface during cooling and that this oxygen species passivates the surface and inhibits further oxidation [9]. Salomonsson *et al.* [8]

explained the hysteresis in the terms of equilibrium in a three-phase system: gas phase O_2 and two solid phases, Pd and PdO_x. A more complex four-phase scheme proposed by Wolf *et al.* [10] includes Pd metal, PdO bulk, surface PdO and chemisorbed oxygen.

The literature review leads to the straightforward conclusion that the catalytic activity of palladium in hydrocarbon oxidation reactions depends on the oxygen-palladium chemistry. The interaction of palladium with oxygen has been studied extensively under low pressure conditions (< 10^{-6} mbar), (see e.g. [11-18] and refs. therein). On the Pd(111) surface, adsorption of O_2 at room temperature (RT) results in a (2×2) O_{ads} structure with a coverage of 0.25 ML [11, 15, 16]. An incommensurate two-dimensional surface oxide, Pd_5O_4, forms after exposure of the (111) surface to O_2 at 600 K as reported by Lundgren *et al.* [19]. Diffusion of oxygen into the palladium bulk was supposed to occur at high temperatures [11-13, 15, 17]. Oxygen dissolved in the bulk is suggested to form a Pd-O solid solution [12] and desorbs above 1100 K [11, 15]. Recently, Yudanov *et al.* [20] computed kinetic barriers for surface-bulk migration of C, N, and O atoms. From their calculations one can estimate that diffusion of oxygen in the bulk becomes appreciable above 900 K.

The pressure difference, often referred to as a pressure gap, prevents to apply the atomic-level knowledge obtained by surface science to real catalytic reactions carried out at atmospheric pressure. However, one should keep in mind that with increasing pressure, the thermodynamic limit changes and new reaction channels can appear while the surface reconstructs. These processes exhibit pressure threshold, which can be in the millibar partial pressure regime. This is relatively "high-pressure" for surface science. Under high yield catalytic conditions, for instance, the oxygen chemical potential to be expected to oscillate around the threshold value for phase formation and the processes involved in kinetically controlled phase transformations are directly relevant for practical catalytic behaviour. In order to understand a real dynamic system, *in-situ* investigations are needed, but the problem is that surface sensitive techniques typically operate only under high-vacuum conditions. However, due to a recent breakthrough in instrument development, specific surface science techniques can now be used at elevated pressures. For instance, X-ray photoelectron spectroscopy (XPS) is able to operate at pressures of up to several mbar (see for instance [21] and references therein).

In this paper we represent the first *in-situ* XPS investigation of oxygen interaction with palladium at elevated pressure. The adsorbed species and the surface chemical states were monitored *in situ* during oxygen exposure. An in-situ measurement is very crucial for understanding the dynamic response of the oxygen/palladium system. For instance, at 1 mbar O_2, PdO is thermodynamically stable up to approximately 840 K, but in 10^{-6} mbar O_2 the stability limit is only approximately 610 K. This means that in a study of palladium oxidation by surface science techniques at elevated pressure the way of quenching the reaction becomes critical, but *in-situ* investigations overcome this problem. Variation of the photon energy allows us to investigate the depth distribution of the oxygen species and the oxidised states of palladium. The information depth is proportional to the inelastic mean free path of the photoelectrons, which depends on their kinetic energy [22]. The photoelectron kinetic energy can be varied by changing the photon energy. A non-destructive depth profiling experiment addressed the questions on oxygen diffusion into the bulk and on bulk palladium oxidation.

2. Experimental

The experiments were performed at beamline U49/2-PGM2 at BESSY in Berlin. The high-pressure XPS setup is described elsewhere [21]. The binding energy (BE) was calibrated with respect to the Fermi edge. The spectral resolution was 0.1 eV at photon energy of 500 eV.

The sample, a (111)-oriented Pd single crystal, was mounted on a temperature-controlled heating stage. The temperature was measured by a chromel-alumel thermocouple spot-welded onto the side of the sample. The sample was heated by the IR laser from the rear, limiting the heated area strictly to the catalytically active material in the chamber. The sample cleaning procedures consisted of repeated cycles of Ar^+ sputtering at room and elevated temperatures, annealing at 950 K in UHV, and exposure to O_2 followed by flashing at 950 K for 60 seconds in UHV. The sample cleanness was checked by XPS.

The Pd(111) single crystal sample was positioned inside a high-pressure cell at a distance of 2 mm from the 1 mm aperture, used as the limiter and focal point for the differentially pumped electrostatic lens system transferring the photoelectrons without chromatic aberration to the hemispherical analyser (SPECS). The typical heating/cooling rate was 10 K/min.

Surface concentrations of oxygen species were calculated by measuring the ratio between the areas of the O 1s and Pd 3p peaks. The O 1s/Pd 3p area ratio for the 2D oxide phase measured at the photon energy of 650 eV was taken as a calibration value. Oxygen coverage for the 2D oxide phase was assumed to be 0.58 ML [19]. For the O 1s/Pd 3p region measured with the other photon energy during the depth profiling experiments, the O 1s/Pd 3p ratio was corrected on the photon-energy dependence of the atomic subshell photoionization cross sections for O 1s and for Pd 3p [23].

3. Results

3.1. In situ XPS characterisation of the 2D oxide

Figure 1 shows the O 1s/Pd3p and Pd $3d_{5/2}$ spectra, which were collected from on the Pd(111) surface heated in 2×10^{-3} mbar O_2 to 571 K and to 598 K. The main problem in XPS analysis of the oxygen/palladium system is the

Table 1: XPS characteristic of the oxygen species. Photon energy 650 eV.

a) Heating in 2×10^{-3} mbar O_2

XPS peak	Assignment	O 1s	
		BE, eV	FWHM
O (I)	2D oxide, Pd_5O_4	528.92 ± 0.05	0.91 ± 0.11
O (II)	2D oxide, Pd_5O_4	529.52 ± 0.05	0.94 ± 0.09
O (III)	Supersaturated O_{ads} layer with coverage of 0.5 ML	530.38 ± 0.07	1.18 ± 0.19

b) Cooling in 2×10^{-3} mbar O_2

XPS peak	Assignment	O 1s	
		BE, eV	FWHM
O (I)	2D oxide, Pd_5O_4	528.96 ± 0.03	0.93 ± 0.13
O (II)	2D oxide, Pd_5O_4	529.58 ± 0.05	0.89 ± 0.06
O (III)	Supersaturated O_{ads} layer with coverage of 0.5 ML	-	-

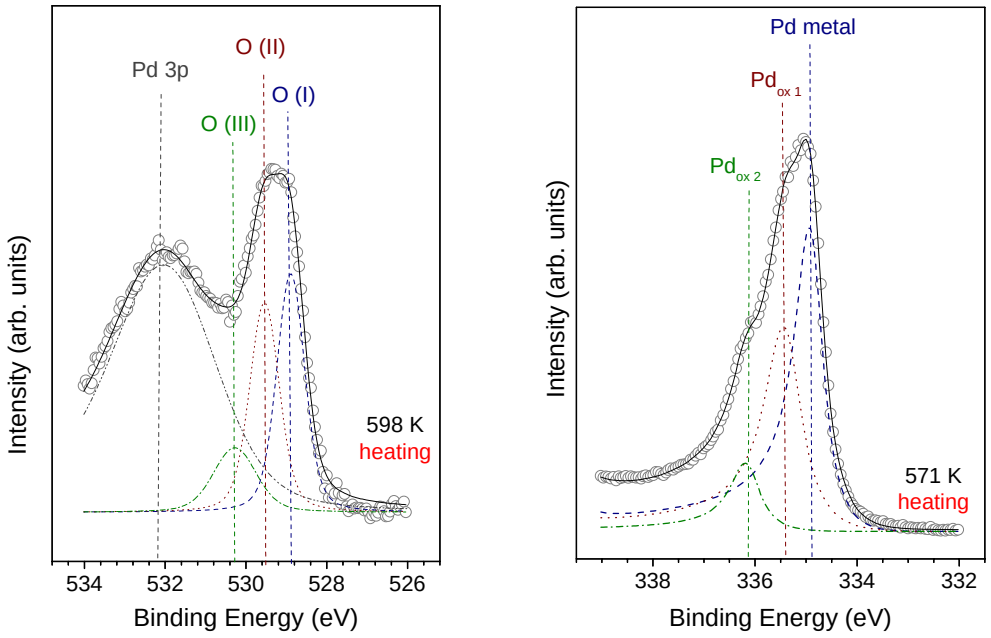

Figure 1: O 1s/Pd3p (the left panel) and Pd $3d_{5/2}$ (the right panel) spectra collected from the 2D oxide on the Pd(111) surface in 2×10^{-3} mbar O_2. The spectra were acquired at 571 K and at 598 K. The photon energy was 460 eV and 650 eV for the Pd 3d and O 1s regions, respectively.

overlap between the O 1s and Pd $3p_{3/2}$ peaks. The analysis suggested in the literature [15, 19] is based on the subtraction of the Pd $3p_{3/2}$ peak obtained from the clean Pd(111) surface from the spectra obtained after oxygen exposure. During our *in situ* experiments, the position of Pd $3p_{3/2}$ peak and its Full Width at Half Maximum (FWHM) were found to change upon heating/cooling in oxygen. In addition a plasmon resonance was excited, with a binding energy (BE) approximately 6 eV higher than the palladium peaks (not shown in Figures). The intensity of this plasmon and its position also change depending on the oxidised states. Therefore, the subtraction of the Pd $3p_{3/2}$ peak for clean Pd(111) from the spectra taken *in situ* was not a reliable procedure. In our case, the O 1s/Pd 3p region was directly fitted with five components, i.e. the O(I), O(II) and O(III) components for the O 1s signal were complemented with Pd $3p_{3/2}$ and plasmon contributions (not shown in the Figures).

The line shape was assumed to be a Doniach-Sunjic function [24]. The relative ratio of the peaks of the Pd 3d doublet was fixed during the fitting, whereas the other parameters such as intensity, FWHM and peak position were allowed to vary within a reasonable range. Another difference between the curve-fitting procedure used in this paper and those reported before [15, 19] is that both spin-orbital momentum peaks of the Pd 3d doublet were included in the

Table 2: XPS characteristic of the oxidised states of palladium. Photon energy 460 eV.
a) Heating in 2×10^{-3} mbar O_2

XPS peak	Assignment	Pd $3d_{5/2}$ peak		Pd $3d_{3/2}$ peak		Δ = BE(Pd $3d_{5/2}$) - BE(Pd $3d_{3/2}$), eV
		BE, eV	FWHM, eV	BE, eV	FWHM, eV	
Pd metal	Metal	334.88 ± 0.01	0.72 ± 0.1	340.25 ± 0.02	0.67 ± 0.07	5.26 ± 0.01
Pd_{ox1}	2D oxide, Pd_5O_4	335.5 ± 0.01	0.81 ± 0.08	340.75 ± 0.02	0.8 ± 0.07	5.25 ± 0.03
Pd_{ox2}	2D oxide, Pd_5O_4	336.24 ± 0.01	0.59 ± 0.04	341.55 ± 0.03	0.71 ± 0.01	5.31 ± 0.02

b) Cooling in 2×10^{-3} mbar O_2

XPS peak	Assignment	Pd $3d_{5/2}$ peak		Pd $3d_{3/2}$ peak		Δ = BE(Pd $3d_{5/2}$) - BE(Pd $3d_{3/2}$), eV
		BE, eV	FWHM, eV	BE, eV	FWHM, eV	
Pd metal	Metal	334.98 ± 0.01	0.67 ± 0.07	340.25 ± 0.01	0.67 ± 0.05	5.27 ± 0.01
Pd_{ox1}	2D oxide, Pd_5O_4	335.44 ± 0.02	0.8 ± 0.07	340.72 ± 0.02	0.85 ± 0.09	5.28 ± 0.01
Pd_{ox2}	-	-	-	-	-	-

fitting. Therefore, the Pd 3d spectra were fitted by three pairs of components for Pd 3d and one pair for plasmon excitation.

The peak positions and the FWHMs of the oxygen species and the oxidised palladium states are summarised in Table 1 and Table 2. The oxygen species assignment was based on the available literature data [15, 19]. According to Ref. [19], the 2D oxide, Pd_5O_4, is characterised by O 1s components at approximately 529 eV with a BE shift of 0.75 eV and an intensity ratio close to 1:1. In our case as shown in Table 1, the O(I) and O(II) components at 528.92 eV and 529.52 eV demonstrated a shift of 0.60 eV, which is close to the theoretically predicted value of 0.51 eV for two different types of oxygen atoms belonging to Pd_5O_4 [19]. Two oxygen-induced Pd $3d_{5/2}$ components, shifted towards higher BE by 0.62 eV and 1.3 eV with respect to the metal peak, were reported for the 2D oxide [19]. This is in good agreement with our observations (Table 2).

Leisenberger *et al.* [15] assigned the O 1s peaks at 529.2 eV and 531.2 eV to atomic oxygen and CO adsorbed on Pd(111), respectively. In our experiments the O 1s peak at 531.2 eV was not observed but, on the other hand, the O 1s component at 530.37 eV was detected. Tentatively the O(III) peak at 530.37 eV was assigned to a compressed oxygen adlayer with a coverage beyond 0.25 ML. This assignment will be considered in more detail in the Discussion Section.

Summarising, the O(I) and O(II) components at 528.92 eV and 529.52 eV were assigned to two types of oxygen atoms from the 2D oxide. The two Pd 3d components at 335.5 eV and 336.24 eV were also attributed to the 2D oxide.

3.2. Heating in oxygen

Figure 2 represents sets of O 1s/Pd 3p and Pd $3d_{5/2}$ core level spectra obtained *in situ* during heating the Pd(111) surface in 2×10^{-3} mbar O_2. The photon energy for measurements of the O 1s/Pd 3p and Pd 3d core levels was 650 and 460 eV, respectively. The photon energy was chosen to set the kinetic energy of photoelectrons in the range of 120 eV and, by doing so, to provide better surface sensitivity. A number of spectral transformations occurred during heating. The O 1s/Pd 3p spectra obtained at temperatures below 476 K show a broad poorly resolved feature, consisting of the O(I), O(II), O(III) and Pd $3p_{3/2}$ components (the left panel in Figure 2). Two oxygen-induced components, Pd_{ox1} and Pd_{ox2}, were distinguished in the Pd 3d spectra (the right panel in Figure 2). These observations indicate the 2D oxide forming at relatively low temperatures. It should be noted that under low pressure conditions the Pd_5O_4 phase appears above 500 K [25]. The oxygen coverage assigned to the 2D oxide was estimated to be approximately 0.37 ML; however according to the literature [19], the local coverage of Pd_5O_4 should be 0.58 ML. This might reflect a state of the surface, in which a fraction of the surface was covered by the 2D oxide and a residual fraction was covered by a rather dense O_{ads} layer (coverage > 0.25 ML). The coverage of the dense O_{ads} layer is estimated to be approximately 0.5 ML. The formation of

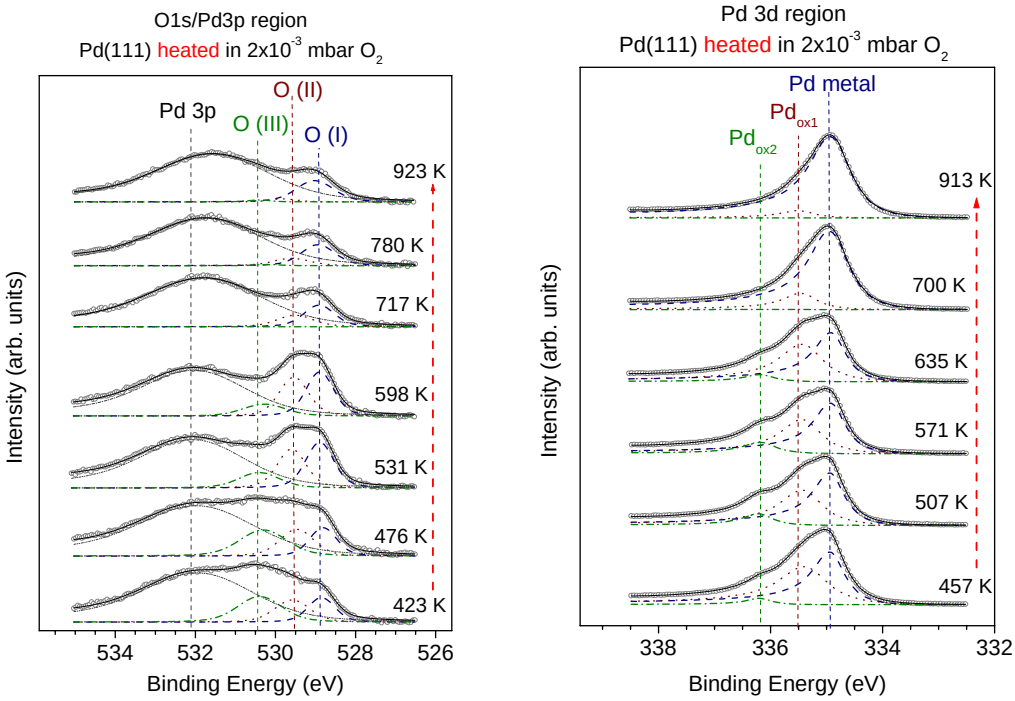

Figure 2: O 1s/Pd 3p and Pd $3d_{5/2}$ spectra collected from the Pd(111) surface during heating in 2×10^{-3} mbar O_2. The photon energy was 650 eV and 460 eV, respectively.

the dense O_{ads} layer was induced by the high oxygen chemical potential (see Discussion). Chemisorbed oxygen in the well-known p(2×2) structure (0.25 ML) is characterised by an O 1s peak at 529.2 eV [15], which should mainly overlap with the O(I) component. The presence of major amounts of (2×2) O_{ads} would thus change the ratio between the O(I) and O(II) peaks. However, the O(I)/O(II) ratio was observed to be close to unity (0.8-0.9) as expected for the 2D oxide and, therefore, the presence of major amounts of (2×2) O_{ads} can be ruled out at this stage.

During heating up to 600 K, the O(III) component decreased and disappeared completely, whereas the intensity of the O(I) and O(II) components at 528.92 eV and 529.52 eV increased by a factor of 1.6 and their ratio remained approximately unity (Figure 3). These changes were associated with growth of the 2D oxide phase from the dense chemisorbed adlayer. The coverage of the 2D oxide was estimated to be 0.58 ML. The shape of the Pd 3d signal changed only slightly upon heating to 600 K (Figure 2). The Pd_{ox2} state was suppressed in the beginning but then the ratio between Pd_{ox2}/Pd_{ox1} reached a value of 0.27 at 571 K. Interestingly, the total contribution of the oxygen-induced Pd components remained constant up to approximately 700 K (Figure 4) as expected for a surface oxide. The presence of O_{ads} did not significantly alter the fitting of the Pd 3d spectra because the O_{ads}-induced components are expected to overlap with the 2D-oxide-originated peaks. We used only two high BE components in fitting the Pd 3d region and, therefore, the O_{ads}-induced peak might contribute to the Pd_{ox1} state.

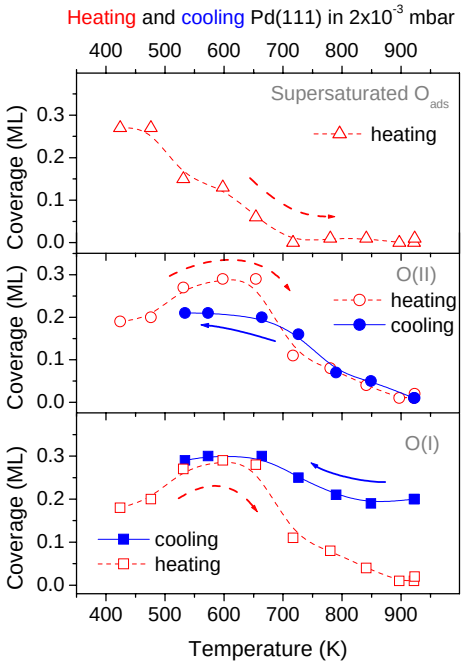

Figure 3: Coverage of oxygen species on the Pd(111) surface as a function of temperature during heating and cooling in 2×10^{-3} mbar O_2. The relative error is estimated to be 14%.

The O 1s/Pd 3p and Pd 3d spectra observed around 600 K were very similar to those reported by Lundgren *et al.* [19] for the two-dimensional oxide, Pd_5O_4. The *in situ* XPS experiment showed that the 2D oxide formed completely upon heating the Pd(111) surface in 2×10^{-3} mbar O_2

at approximately 600 K. Again the 2D oxide was characterised by the O(I) and O(II) components with a ratio of approximately 1:1 and by the Pd_{ox1} and Pd_{ox2} components with a ratio of approximately 4:1.

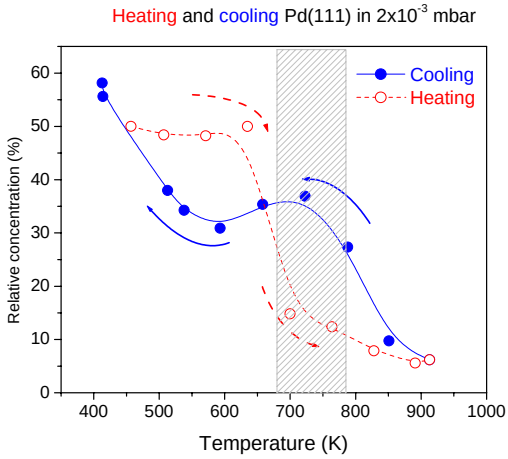

Figure 4: Variation of the oxidised states of the Pd(111) surface during heating and cooling in 2×10^{-3} mbar O_2. The concentration was calculated from the Pd 3d spectra shown in Figure 2 and Figure 5. The concentration was normalised on the total Pd 3d signal. The relative error is estimated to be 10%.

The coverage of oxygen species and the relative concentration of the oxidised palladium states are plotted in Figure 3 and Figure 4 as a function of temperature. The thermal stability of the 2D oxide can be followed by monitoring either the O(I)/O(II) species (Figure 3) or the oxidised states of palladium (Figure 4). The 2D oxide started to decompose between 655 K and 700 K, which was manifested by the sharp decrease of the amount of O(I)/O(II) species and of the Pd_{ox1} and Pd_{ox2} components. It is quite remarkable that the O 1s peak was observed after Pd_5O_4 decomposition. A substantial oxygen signal was detected even at 925 K, whereas no oxidised states of palladium were observed at this temperature. Also, as the 2D oxide decomposes, the O(I) peak shifts slightly towards high BE to 528.98 eV. The highly stable oxygen species cannot be due to surface segregation of impurities such as Si, which forms stable oxides. Survey spectra were recorded frequently, which did not show evidence of any impurities. Moreover, the oxygen signal became zero when oxygen was pumped out and this would not be the case for SiO_2 segregation. The highly stable oxygen species can be associated with oxygen migration and dissolution into the palladium bulk. Both theoretical [20, 26] and experimental investigations [15] suggested that the rate of oxygen migration in the bulk becomes appreciable at this temperature, due to the high activation barrier for diffusion through the first atomic layer. Indeed, the observed oxygen peak cannot be explained by the presence of chemisorbed oxygen or of the 2D oxide or of Pd phase. The temperature was well above the desorption temperature of chemisorbed oxygen, which was reported to be approximately 750 K [15]. According to the study by Zheng *et al* [16], PdO should decompose at even lower temperatures than chemisorbed oxygen desorbs. Yudanov *et al*. [20] suggested a progressive population of bulk or interstitial binding sites by oxygen from an existing oxygen surface coverage. From the viewpoint of statistical thermodynamics, at high temperatures the balance between surface and bulk populations should be changed in favour of bulk binding sites.

Since oxygen atoms incorporated into the 2D oxide, O(I), and dissolved oxygen species are spectroscopically undistinguishable, the addition of a component for the dissolved oxygen species in the curve-fitting procedure was not reasonable. Anyway, careful analysis of the *in situ* XPS data allowed us to follow oxygen dissolution as described in the Discussion Section.

Summarising the *in situ* XPS measurements in 2×10^{-3} mbar O_2 during heating the Pd(111) surface, one can conclude:

1. The 2D oxide exists already at 423 K, covers the entire surface at 654 K and the Pd_5O_4 phase decomposes above 700 K. Pd_5O_4 is characterised by (a) the O(I) and O(II) components at 528.92 eV and 529.52 eV, respectively, with a ratio of approximately 1:1, and (b) the Pd_{ox1} and Pd_{ox2} components at 335.5 eV and 336.24 eV, respectively, with a ratio of approximately 4:1.
2. Decomposition of the 2D oxide is followed by oxygen dissolution into the bulk. The O 1s core level peak at 528.98 eV was observed even at 925 K. The dissolved oxygen is of atomic nature likely without forming a strong interaction with the Pd-d band giving rise to a solid solution scheme with a metallic state and oxygen. The oxygen-palladium interaction might be different from an oxide nature where a substantial charge transfers from Pd to oxygen.

3.3. Cooling in oxygen

Figure 5 shows the sets of O 1s/Pd 3p and Pd $3d_{5/2}$ core level spectra obtained *in situ* during cooling the Pd(111) surface in 2×10^{-3} mbar O_2. The cooling experiment was performed immediately after heating the Pd(111) single crystal in oxygen. The O 1s/Pd 3p spectrum obtained at 923 K exhibits a single oxygen peak, which was assigned to dissolved oxygen species. The metallic component was mainly detected in the Pd 3d region at 913 K and almost no oxygen-induced components were observed.

Cooling to 850 K resulted in no changes in the O 1s/Pd 3p and Pd 3d spectra. However, further cooling led to the growth of the O(I) and O(II) components along with the Pd_{ox1} peak at 335.44 eV. Very remarkable findings are that, on the one hand, the oxidised state of palladium is clearly different from the Pd_5O_4 phase formed during heating and, on the other hand, it appeared at higher temperature than the temperature of Pd_5O_4 oxide decomposition. The hysteresis behaviour in oxidation is evident in Figure 4. The width of the hysteresis window is approximately

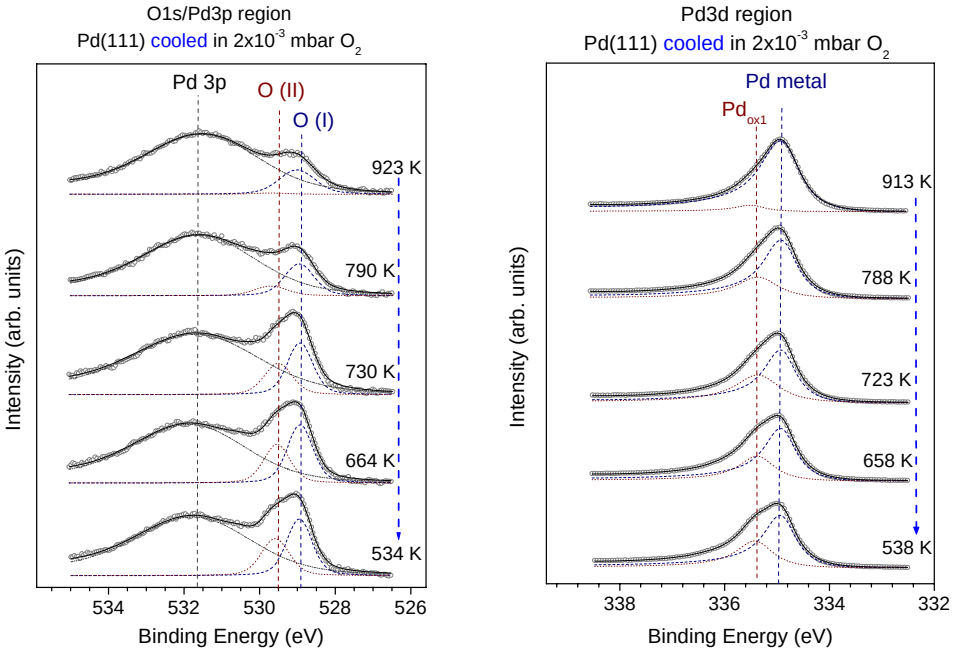

Figure 5: O 1s/Pd 3p and Pd $3d_{5/2}$ spectra collected from the Pd(111) surface during cooling in 2×10^{-3} mbar O_2. The photon energy was 650 eV and 460 eV, respectively.

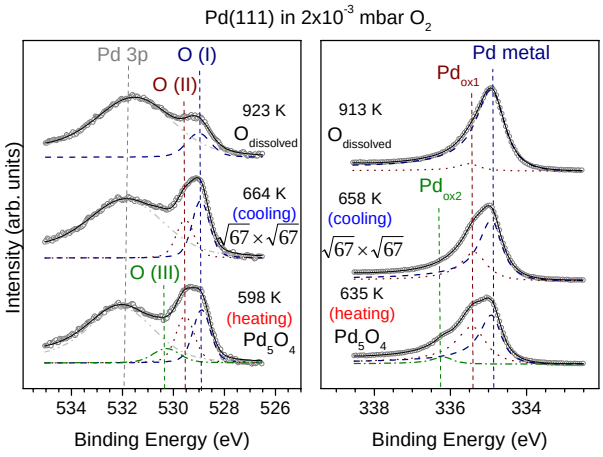

Figure 6: O 1s/Pd 3p and Pd 3d spectra of the 2D oxide, the $(\sqrt{67}\times\sqrt{67})$R12.2° phase and the dissolved oxygen species. O 1s/Pd 3p and Pd 3d spectra collected at photon energies of 650 eV and 460 eV, respectively.

60-70 K. The Pd 3d core level spectra obtained from the new oxide state are different from those of the Pd_5O_4 oxide. Both the new phase and Pd_5O_4 are characterised by two oxygen components with similar BE, but the new phase shows only one high BE peak in the Pd $3d_{5/2}$ spectra, where as the 2D oxide exhibits two components, Pd_{ox1} and Pd_{ox2}. The absence of the Pd_{ox2} component cannot be explained by a fitting error: the Pd_{ox2} shoulder was clearly visible in the Pd 3d spectra obtained during heating. The ratio between the O(I) and O(II) components was approximately 1.4, and this value is noticeably higher than the 1:1 ratio observed during heating. One might argue that the contribution of the bulk dissolved oxygen component causes the change in the O(I)/O(II) ratio. However, the recent STM and TPD work on the oxidation of Pd(111) at pressures around 10^{-5} mbar at 700 K [25] revealed the formation of a previously unknown hexagonal surface oxide phase $(\sqrt{67}\times\sqrt{67})$R12.2° with oxygen coverage of only approximately 0.4 ML. This hexagonal surface oxide phase was stable at somewhat higher temperatures than the Pd_5O_4 oxide phase and acted as an intermediate for Pd_5O_4 growth. It is composed of uniform oxide clusters, which may, in contrast to Pd_5O_4, contain only equivalent Pd atoms. In our case, oxygen coverage for the new phase was estimated to be 0.48 ML. This value is slightly lower than the corresponding number for the Pd_5O_4 phase. These facts are in good agreement with data reported in Ref. [25].

For a better representation, the core level spectra for Pd_5O_4, new hexagonal $(\sqrt{67}\times\sqrt{67})$R12.2° phase and dissolved oxygen are shown in Figure 6. The main results of the *in situ* XPS measurements during cooling in 2×10^{-3} mbar O_2 are:

1. The oxidised state of palladium during cooling appeared at higher temperatures than the temperature of the 2D oxide decomposition.
2. The oxide phase formed during cooling was not identical to the 2D oxide and may be attributed to a recently discovered hexagonal surface oxide phase [25].

3.4. In situ depth profiling

In order to verify the surface nature of the 2D oxide, O 1s/Pd $3p_{3/2}$ and Pd 3d spectra were taken with different

photon energies as shown in Figure 7. The spectra were obtained *in situ* in 2×10^{-3} mbar O_2 at 603 K. An increased photon energy results in an increased kinetic energy of photoelectrons and consequently the information depth increases. Thus, the spectra obtained at low photon energy are more surface sensitive, whereas the spectra obtained at high photon energy contain essentially bulk contribution. Figure 8 shows the ratio between O 1s and Pd $3p_{3/2}$ peaks as a function of information depth. It is remarkable that the O 1s/Pd 3p ratio and the concentration of the oxidised Pd states dropped off with increasing information depth (Figure 8). These facts allow us to draw the straightforward conclusion that the 2D oxide is located at the surface.

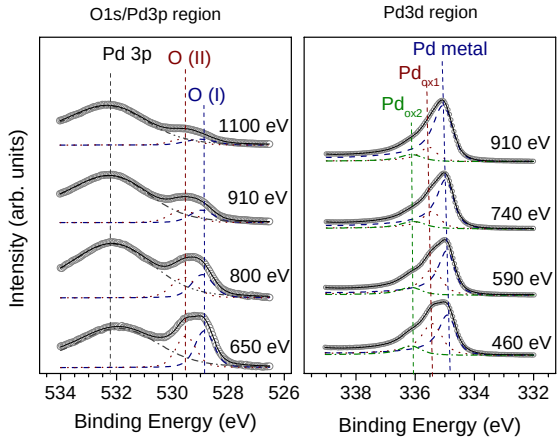

Figure 7: Depth profiling of the 2D oxide. The XPS spectra were obtained in-situ at 603K in 2×10^{-3} mbar O_2 with photon energy specified.

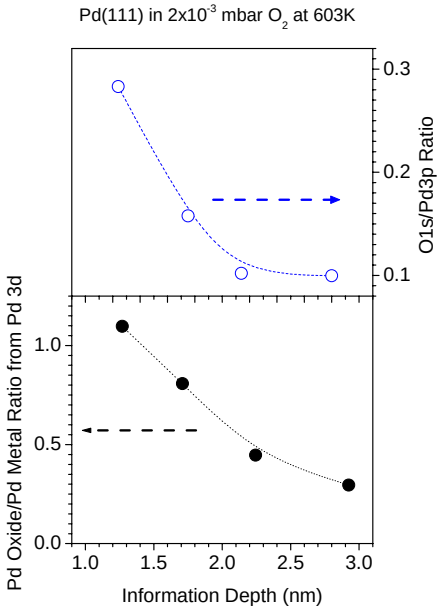

Figure 8: The O 1s/Pd 3p ratio and the oxidised states of palladium as a function of information depth. The ratio was calculated from the spectra shown in Figure 7.

With respect to the Pd 3d peaks, it should be mentioned that the metallic component at 334.88 eV slightly shifted to 335.00 eV when the photon energy was varied from 460 eV to 910 eV. This reflects the increase of the contribution of the bulk component with increase of the information depth. Indeed, Pd(111) was estimated to have 0.28 eV surface core-level shift, which is the core-level difference between an atom at the surface and in the bulk [27]. Due to the small value of the surface core-level shift it is not worth to include additional components representing the surface or the bulk. On the other hand, the surface core-level shift manifested itself by the high BE shift of the metallic component when the contribution of the bulk increased. The same high BE shift of the Pd 3d peaks was observed for the clean Pd(111) surface when the photon energy was varied.

The dissolved oxygen species was also studied by varying the photon energy. The O 1s/Pd3p core level spectra were obtained *in situ* in 2×10^{-3} mbar O_2 at 793 K as shown in Figure 9. The main contribution to the O 1s signal was the peak at 528.99 eV, which had been assigned to dissolved oxygen. The oxygen contribution compared to the Pd $3p_{3/2}$ peak did not change with increasing information depth (the right panel in Figure 9). This fact unambiguously points that at elevated temperatures oxygen dissolves in the palladium bulk. The dissolved oxygen species is characterised by the O 1s core level peak at 528.99 eV.

4. Discussion

The experimental results presented above demonstrate that the interaction of palladium and oxygen passes several distinct steps and depends on the sample prehistory. Voogt *et al.* [14] did not observe the surface oxide at room temperature in 10^{-5} mbar O_2 on Pd(111) and on palladium foil, but that the surface oxygen coverage increased slowly up to 1 ML resulting in a (1×1) LEED structure, which probably was indeed due to very disordered surface oxide. These authors [14] also proposed three stages in the interaction of oxygen with Pd(111) at elevated temperatures (>470 K) and pressures above 10^{-6} mbar. The first stage is the dissociative adsorption of oxygen on the surface resulting in a coverage of 0.25 ML, corresponding to the p(2×2) chemisorbed oxygen structure. During the second stage oxygen atoms diffuse into the surface structure with a local coverage close to 0.5 ML. The third stage, nucleation and growth of the surface oxide with coverage of 0.5 ML, was considered to be a phase transition without significant change in oxygen coverage. Recently, a combined TPD and STM study by Gabasch *et al.* [25] showed that in the 10^{-6} to 10^{-5} mbar range at 673 K, Pd_5O_4 formation occurs indeed in several steps: (i) p(2×2) formation; (ii) diffusion of additional O atoms into the terraces up to 0.4 ML coverage and formation of a disordered surface oxide; (iii) ordering to form a hexagonal phase at 0.4 ML and (iv) additional uptake of oxygen up to ~0.6 ML and

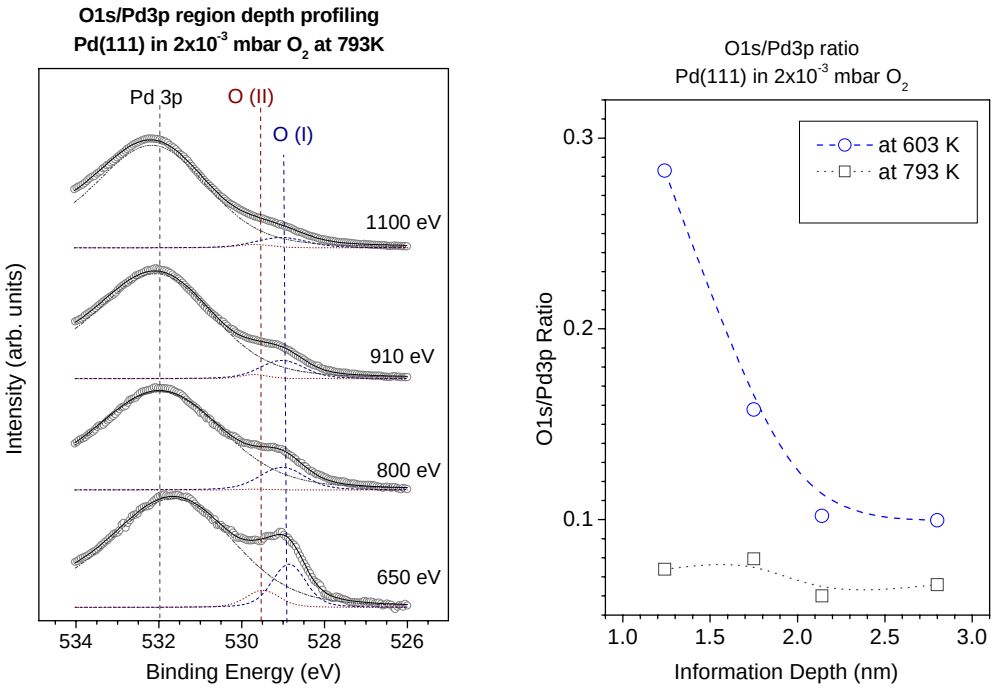

Figure 9: The left panel: the O 1s spectra observed in-situ in 2×10^{-3} mbar O_2 at 793 K. The right panel: O 1s/Pd 3d ratio for the dissolved oxygen species and for the 2D oxide as a function of information depth.

surface rearrangement to the square Pd_5O_4 surface oxide.

Our present experiments were performed at an O_2 pressure of 2×10^{-3} mbar, considerably higher than used in Refs. [14, 25] and, therefore, Stage 1 was quickly surpassed. Our observations rather started at Stage 2, however, our interpretation of this stage is different from that proposed in [14]. The DFT calculations [26] predicted a 0.5 ML oxygen adlayer as a "precursor" of the surface oxide. In support of this prediction, we observed the O 1s peak, O(III), at 530.38 eV, which was assigned to the compressed O_{ads} layer with an equilibrium coverage estimated to be approximately 0.5 ML. An alternative explanation of the O(III) peak could be a disordered surface oxide, as reported in Ref. [25]. According to Ref. [25], the disordered surface oxide might be a precursor for the 2D oxide. On the other hand, the disordered oxide covers the surface only partially at around 500 K and is limited to the step edges. Therefore, although none of the apparent possibilities - disordered surface oxide or the compressed O_{ads} layer, or even their coexistence - can be ruled out on the basis of the presented experimental data, we rather prefer to assign the O(III) peak to a compressed O_{ads} layer. Such a situation has been considered in related DFT calculations [19], showing that the binding energy of O_{ads} in a 0.5 ML p(2x1) adlayer is not very much lower than of oxygen in the surface oxide. At low temperatures such adlayers may represent “metastable” states due to kinetically limited mass transport. Klötzer *et al.* [28] reported that the formation of the surface oxide is blocked below 423K. Moreover, the temperature of 423K was just the kinetic limit where the TPD feature of the oxide started to appear [28]. Surface oxide nucleation starts only if a sufficient supersaturation beyond 0.25 ML is achieved [25]. These facts are consistent with *in situ* XPS data where the co-existence of the 2D oxide and the supersaturated oxygen structure was found. It is reasonable to assume that under high pressure conditions the dynamic adsorption-desorption equilibrium might be shifted from the (2×2) structure towards a denser O_{ads} layer. According to XPS data (Figure 2), the denser O_{ads} layer co-exists with the 2D oxide in 2×10^{-3} mbar O_2 at 423 K.

The assignment of the O(III) peak with the BE of 530.38 eV to the denser O_{ads} layer looks reasonable from the following point of view. The p(2×2) O_{ads} layer with a coverage of 0.25 ML is characterised by the O 1s peak at 529.2 eV [15] and CO_{ads} shows the O 1s peak at 531.2 eV [15]. The difference demonstrates that the oxygen state in CO_{ads} is more “electrophilic” than chemisorbed oxygen, which draws electron density from the Pd metal. Increase of the oxygen coverage beyond 0.25 ML should result in reduced electron transfer from metal to oxygen and, therefore, the dense O_{ads} layer with coverage 0.5 ML could be characterised by the peak at the lower BE of 530.38 eV. The O 1s peak at 530.38 eV is not a feature of CO_{ads}: CO_{ads} readily reacts with oxygen below 425 K [15].

During Stage 3, the contribution of the supersaturated O_{ads} layer decreased with temperature and dropped down to zero above 654 K, whereas the signal from the 2D oxide grew and reached a maximum between 600 K and 654 K (Figure 2 and Figure 3). However, the weak O(III) peak was detected even at 654 K. This might reflect “quasi-equilibrium” between the 2D oxide phase and the supersaturated O_{ads} layer. The depth profiling by variation of the

photon energy (Figure 7 and Figure 8) confirmed the surface nature of the 2D oxide. Both O(I) and O(II) were equally losing intensity with increasing photon energy and - in other words - with increasing the information depth. The oxygen-induced component in the Pd 3d signal showed the same behaviour. The consistency in the behaviour of all peaks, O(I) and O(II) alone with Pd_{ox1} and Pd_{ox2}, also supports (i) the peaks assignment to the 2D oxide and, indirectly, (ii) the viability of our spectra fitting procedure.

The 2D oxide started to decompose above 654 K. Remarkably, the ratio between the O(I) and O(II) components was changing during 2D oxide decomposition. The O(I) component was shifting towards slightly higher BE up to 528.98 eV. Moreover, the O(I) peak was a major contributor to the O 1s signal above 780 K. The O 1s peak at 528.98 eV was quite intensive even at 923 K. This temperature is well above the desorption temperature of the chemisorbed oxygen species [15, 16, 28] and much higher than the temperature of PdO decomposition [16]. Therefore we assigned the peak at 528.98 eV to the oxygen atoms dissolved in the palladium bulk. This assignment was supported by the depth profiling by varying photon energy (Figure 9). With increasing information depth the peak of dissolved oxygen species lost intensity relative to Pd $3p_{3/2}$. This was in contrast with the sharp decrease of the O 1s/Pd 3p ratio for the 2D oxide. The 2D oxide peaks decreased threefold when the photon energy changed from 650 eV to 1100 eV and the information depth decreased from 1.2 nm to 2.8 nm. The existence of a concentration gradient of dissolved oxygen perpendicular to the surface cannot be ruled out; however, the gradient changes should occur deeper than the XPS information depth. Diffusion into the bulk is temperature-dependent and this might result in a progressively steeper concentration gradient at lower temperatures. The diffusion limit of oxygen transportation both through the surface and inside the metal bulk is extremely important for understanding the palladium-oxygen system [20]. Experimentally, palladium oxidation at high pressure (>10 mbar) at 600 K was found to be controlled by diffusion of oxygen into the palladium bulk [29].

No essential contribution of the oxygen-induced components was found in the Pd 3d spectra when the dissolved oxygen species in equivalent of 0.2 ML was present in the bulk. This might rather be reasonable for a solid solution of oxygen in the palladium bulk. First, the oxygen concentration in the solid solution is lower than that in any oxide phase. So, the concentration of oxygen-induced Pd might be just below the detection limit. The concentration of dissolved oxygen was estimated to be less than 0.1 ML per palladium layer. Second, electron density transfer from the oxygen-neighbour palladium atom to oxygen might be compensated through electron density donation from the surrounding palladium atoms, which do not neighbour to oxygen. This might be easier to achieve for the solid solution. It should be noted that at low concentration of the dissolved oxygen species the transfer of electron density from the non-oxygen-bonded palladium might also be facilitated.

The O(I) peak of the 2D oxide has a BE very close to the peak of the dissolved oxygen species and, therefore, the addition of the component for the dissolved oxygen to the curve-fitting procedure was not reasonable. However, the quantitative analysis of oxygen dissolution can be extracted from the *in situ* XPS data. One main assumption needs to be made that the ratio between the O(I) and O(II) components of the 2D oxide is constant. In good agreement with [19], our data revealed a ratio of approximately 1:1 at the temperatures below Pd_5O_4 decomposition. Therefore, larger contribution of the O(I) component at the high temperatures can be assigned to the dissolved oxygen species. The corrected concentration of the 2D oxide and the dissolved oxygen species is represented in Figure 10. The correction was done assuming a 1:1 ratio between O(I) and O(II) components and the excess of oxygen was assigned to the dissolved oxygen species. Remarkably, the concentration of dissolved oxygen grew with decomposition of the 2D oxide. Likely, while the 2D oxide decomposes, a new reaction channel for oxygen is opened: diffusion into the palladium bulk. Two explanations can be proposed. First, the 2D oxide serves as a “preservation” layer and prevents oxygen diffusion in the bulk. In the second place, temperature activation might be required to facilitate diffusion.

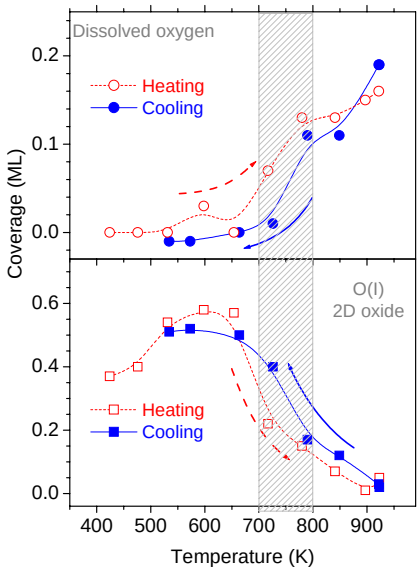

Figure 10: Corrected coverage of oxygen species on the Pd(111) surface as a function of temperature during heating and cooling in 2×10^{-3} mbar O_2. The coverage of O(I) was corrected by subtracting the contribution of the dissolved oxygen species (see the text).

The analysis of Figure 3, Figure 4 and Figure 10 reveals another interesting effect: during the cooling process surface oxidised states of palladium appeared at higher temperatures than the temperature of the 2D decomposition. This phenomenon is clearly assigned to a redox hysteresis and the hysteresis window is indicated in Figure 4 and Figure 10. It reveals a previously unknown aspect of

the well-known Pd redox hysteresis. According to Refs. [5, 9], the decomposition of PdO to Pd and its re-formation give rise to a hysteresis, as palladium oxide heated in oxygen atmosphere decomposes at higher temperatures than it forms back during cooling. The authors of Refs. [5, 9] supposed that strongly bound chemisorbed oxygen is formed on the palladium surface during cooling and this oxygen species passivates the surface and inhibits further oxidation. Our finding allows us to shed some new light on this hypothesis. Previously, it has been shown [25] that the Pd_5O_4 surface oxide phase is formed at a critical oxygen chemical potential in the gas phase, but also that the formation of the hexagonal $(\sqrt{67}\times\sqrt{67})$R12.2° surface oxide phase with lower oxygen content is favoured at a somewhat higher temperature. Our data show that the high-temperature surface oxide phase observed during cooling is different from the 2D oxide observed during heating. Indeed, the oxygen coverage of the new phase is approximately 0.48ML, which reasonably agrees with the 0.4 ML reported by Gabasch *et al.* [25], whereas the 2D oxide coverage is 0.58 ML in Ref. [19]. The 2D oxide is characterized by two Pd $3d_{5/2}$ components at 335.5 eV and 336.24 eV but the new oxide phase shows only one single component at 335.45 eV.

The question why Pd_5O_4 does not form during cooling is open. It is unlikely that there is kinetic limitation of the $(\sqrt{67}\times\sqrt{67})$R12.2° phase transformation into the Pd_5O_4 surface oxide. On the other hand, an oxide phase similar to the Pd_5O_4 surface oxide was observed during cooling in 0.4 mbar O_2 as described in Part 2 [30]. One important factor, which should be taken into account, is that very likely the chemical potential of the palladium surface and of the bulk might change due to oxygen dissolution. As we observed during heating/cooling cycles of the Pd(111) surface in 0.4 mbar O_2, the PdO phase could appear or not depending on the pre-history of the sample, in other words depending on dissolved species. Dissolved species can alter the surface properties and hence stabilise one phase and/or destabilise another. Therefore, dissolved oxygen species can be one of the factors determining the "pre-history" of the sample.

5. Summary

A Pd(111) single crystal was used for an XPS study of palladium oxidation *in situ* during heating and cooling in 3×10^{-3} mbar O_2. It is apparent from this study that it is possible to follow the mechanism of palladium oxidation by *in situ* XPS. This study demonstrates the importance of *in situ* measurements for a detailed characterization of the surface and bulk species/oxidised states formed during the interaction between palladium and oxygen. The main advantage of the *in situ* XPS technique is the opportunity to monitor the oxygen/palladium interaction without quenching the reaction.

The *in situ* XPS technique allows us to trace the development of the surface oxide, chemisorbed and other oxygen species. The 2D oxide and the supersaturated O_{ads} layer were successfully identified. The supersaturated O_{ads} layer was characterized by the O 1s core level peak at 530.37 eV. The 2D oxide, Pd_5O_4, was characterized by two O 1s components at 528.92 eV and 529.52 eV and by two oxygen-induced Pd $3d_{5/2}$ components at 335.5 eV and 336.24 eV. The depth profiling by photon energy variation confirmed the surface nature of the 2D oxide. Dissolution of oxygen at elevated temperatures was identified by the O 1s core level peak at 528.98 eV. The "bulk" nature of the dissolved oxygen species was also verified by depth profiling. A new oxide phase, most likely $(\sqrt{67}\times\sqrt{67})$R12.2° [25], was detected during cooling in 3×10^{-3} mbar O_2. The new oxide phase shows only the Pd $3d_{5/2}$ component at 335.45 eV.

Based on the *in situ* XPS data, the following scenario is proposed:

1. Exposure of the Pd(111) single crystal to 3×10^{-3} mbar O_2 at 423 K led to appearance of the 2D oxide phase, which was in equilibrium with the supersaturated O_{ads} layer. The coverage of the supersaturated O_{ads} layer was supposed to be 0.5 ML.
2. Heating in 3×10^{-3} mbar O_2 resulted in disappearance of the supersaturated O_{ads} layer whereas the fraction of the surface covered with the 2D oxide grew. The surface was completely covered with 2D oxide between 598 K and 654 K.
3. Upon further heating in oxygen the 2D oxide started to decompose and almost disappeared above 717 K. Diffusion of oxygen in the palladium bulk occurred at these temperatures. Substantial amounts of oxygen were detected even at 923 K.
4. Surprisingly, during the cooling ramp in 3×10^{-3} mbar O_2, the oxidised Pd states appeared at higher temperature than the decomposition temperature of the 2D oxide. The surface oxidised states exhibited an inverse hysteresis. An additional oxide phase, probably $(\sqrt{67}\times\sqrt{67})$R12.2°, was detected during cooling.

6. Acknowledgement

This work was supported by the European Community - Research Infrastructure Action under the FP6 "Structuring the European Research Area" Programme (through the Integrated Infrastructure Initiative" Integrating Activity on Synchrotron and Free Electron Laser Science - Contract R II 3-CT-2004-506008). The work was also supported by Enterprise Ireland through International Collaboration Programme (IC/2004/099). DZ received a research scholarship from the Foundation of the University of Limerick. HG acknowledges a grant from the Max Planck Society. We gratefully acknowledge BESSY staff for the support during the beamtime.

7. References

[1] R.B. Anderson, K.C. Stein, J.J. Feenan and L.J.E. Hofer, Ind. Eng. Chem. 53 (1961) 809.

[2] R. Burch, F.J. Urbano and P.K. Loader, Appl. Catal., A 123 (1995) 173.

[3] J.N. Carstens, S.C. Su and A.T. Bell, J. Catal. 176 (1998) 136.

[4] R.S. Monteiro, D. Zemlyanov, J.M. Storey and F.H. Ribeiro, J Catal. 199 (2001) 291.

[5] R.J. Farrauto, M.C. Hobson, T. Kennelly and E.M. Waterman, Appl. Catal., A 81 (1992) 227.

[6] R.J. Farrauto, J.K. Lampert, M.C. Hobson and E.M. Waterman, Appl. Catal., B 6 (1995) 263.

[7] J.G. McCarty, Catal. Today 26 (1995) 283.

[8] P. Salomonsson, S. Johansson and B. Kasemo, Catal. Lett. 33 (1995) 1.

[9] A.K. Datye, J. Bravo, T.R. Nelson, P. Atanasova, M. Lyubovsky and L. Pfefferle, Appl. Catal., A 198 (2000) 179.

[10] M.M. Wolf, H. Zhu, W.H. Green and G.S. Jackson, Appl. Catal., A 244 (2003) 323.

[11] H. Conrad, G. Ertl, J. Kueppers and E.E. Latta, Surf. Sci. 65 (1977) 235.

[12] C.T. Campbell, D.C. Foyt and J.M. White, J. Phys. Chem. 81 (1977) 491.

[13] D.L. Weissman, M.L. Shek and W.E. Spicer, Surf. Sci. 92 (1980) L59.

[14] E.H. Voogt, A.J.M. Mens, O.L.J. Gijzeman and J.W. Geus, Surf. Sci. 373 (1997) 210.

[15] F.P. Leisenberger, G. Koller, M. Sock, S. Surnev, M.G. Ramsey, F.P. Netzer, B. Klötzer and K. Hayek, Surf. Sci. 445 (2000) 380.

[16] G. Zheng and E.I. Altman, Surf. Sci. 462 (2000) 151.

[17] V.A. Bondzie, P.H. Kleban and D.J. Dwyer, Surf. Sci. 465 (2000) 266.

[18] G. Zheng and E.I. Altman, Surf. Sci. 504 (2002) 253.

[19] E. Lundgren, G. Kresse, C. Klein, M. Borg, J.N. Andersen, M. De Santis, Y. Gauthier, C. Konvicka, M. Schmid and P. Varga, Phys. Rev. Lett. 88 (2002) 246103/1.

[20] I.V. Yudanov, K.M. Neyman and N. Rosch, Physical Chemestry and Chemical Physics 6 (2004) 116.

[21] H. Bluhm, M. Hävecker, A. Knop-Gericke, E. Kleimenov, R. Schlögl, D. Teschner, V.I. Bukhtiyarov, D.F. Ogletree and M. Salmeron, J. Phys. Chem. B 108 (2004) 14340.

[22] M.P. Seah, Surface and Interface Analysis 9 (1986) 85.

[23] J.J. Yeh and I. Lindau, Atomic Data and Nuclear Data Tables 32 (1985) 1.

[24] S. Doniach and M. Sunjic, Journal of Physics C 31 (1970) 285.

[25] H. Gabasch, W. Unterberger, K. Hayek, B. Klötzer, C. Klein, M. Schmid, P. Varga and G. Kresse, Surface Science, accepted (2005).

[26] Todorova, Physical Review Letters 89 (2002) 96103.

[27] J.N. Andersen, D. Hennig, E. Lundgren, M. Methfessel, R. Nyholm and M. Scheffler, Physical Review B 50 (1994) 17525.

[28] B. Klötzer, K. Hayek, C. Konvicka, E. Lundgren and P. Varga, Surf. Sci. 482-485 (2001) 237.

[29] J. Han, D. Zemlyanov, G. Zhu and F.H. Ribeiro, (in preparation).

[30] H. Gabasch, W. Unterberger, K. Hayek, B. Klötzer, E. Kleimenov, D. Teschner, S. Zafeiratos, M. Hävecker, A. Knop-Gericke, R. Schlögl, B. Aszalos-Kiss and D. Zemlyanov, (in preparation).